



**Mammalian cell: A unique scaffold for in situ biosynthesis of
metallic nanomaterials and biomedical applications**

| | |
|-------------------------------|--|
| Journal: | <i>Journal of Materials Chemistry B</i> |
| Manuscript ID | TB-REV-07-2018-001955.R1 |
| Article Type: | Review Article |
| Date Submitted by the Author: | 05-Sep-2018 |
| Complete List of Authors: | Rehman, Fawad; Southeast University, Department of Biomedical Engineering; Henan University, Interantional Joint Center for Biomedical Innovations, School of Life Sciences Jiang, Hui; Southeast Univ, State Key Laborotary of Bioelectronics Selke, Matthias; California State University, Los Angeles, Chemistry and Biochemistry Wang, Xuemei; Southeast University, Department of Biomedical Engineering |
| | |



Journal Name

ARTICLE

Received 00th **Mammalian cell: A unique scaffold for in situ biosynthesis of metallic nanomaterials and biomedical applications**
January 20xx,

Accepted 00th **Fawad Ur Rehman^{1,2}, Hui Jiang¹, Matthias Selke³, Xuemei Wang^{1*}**
January 20xx

DOI:
10.1039/x0xx00000x

www.rsc.org/

Production of nanoscale materials often requires the use of toxic chemicals and complex synthetic procedures. A new scaffold has been explored for in situ synthesis of nanomaterials that utilizes natural biological systems in the form of plants, bacteria, fungi, algae and redox-imbalanced mammalian cells and systems. The latter approach has become popular in recent years and has shown some promising results in bioimaging of cancer, as well as inflammatory and neurodegenerative maladies. Biosynthesis of nanoclusters in redox-imbalanced mammalian cells is facile, cost-effective and environmentally friendly with higher biocompatibility, target specificity and lower adverse effects than traditional synthetic approaches. Herein, we describe recent advances in mammalian green in situ biosynthesis for biomedical applications, especially in cancer and neurodegenerative disease theranostics.

1. Introduction

Biomedical applications of nanoscale materials are of great interest for clinical applications. The size of typical nanoscale materials used for biomedical applications usually ranges from 10-100 nm, and in some cases, the size may be up to 300 nm, especially for drug delivery vehicles¹⁻². In the biomedical realm, nanoscale materials are used in tissue regeneration and

engineering, photodynamic therapy, sonodynamic therapy, photothermal therapy, biosensors, theranostics, anti-microbial and nano drug delivery system for various neoplastic and non-neoplastic maladies³⁻⁵. The nanoscale materials biomedical applications are favored due to their size and structural analogy with various cell structures and organelles, i.e., DNA, Ribosomes, Mitochondria, Endoplasmic reticulum, Ligand-receptors, and Antibodies, all of which are having a size range from 2 to 20 nm⁶.

It has been estimated that globally around 1300 new nanomaterials are produced every year⁷, with applications ranging from food additives, cosmetics, drug delivery vehicles, surface coating to biomedical therapeutics⁸. The preparation processes of many of these nanomaterials use various hazardous chemicals, and, furthermore often the pre-synthesized nanoscale materials are highly reactive due to their smaller size and maximum surface electron presence. Hence, there is a significant concern in the health and biomedical

¹State Key Laboratory of Bioelectronics, School of Biological Science and Medical Engineering, Southeast University, Sipailou 2, Nanjing 210096 Jiangsu, People's Republic of China.

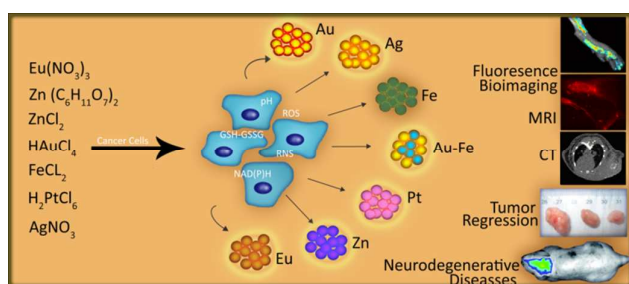
²International Joint Center for Biomedical Innovation, Henan University, Kaifeng, Henan, 457001, China.

³Department of Chemistry and Biochemistry, California State University, Los Angeles, CA 90032, USA

* Corresponding author: xuawang@seu.edu.cn

communities regarding both short-term and long-term exposure to such materials.

Therefore, synthesis of nanoscale materials by plants, bacteria, and fungi, as well as algae has recently become popular⁹. More recently, the eukaryotic, mammalian, neoplastic, pluripotent stem cells and body functional proteins have been found to have some potential for nanoscale materials synthesis. One method is to pre-synthesize highly biodegradable nanomaterials for biomedical applications. Yet another approach, which has recently become popular, involves *in situ* biosynthesis. The *in situ* biosynthesis is comprised of the pre-ionic solutions, i.e. HAuCl₄ (Gold), FeCl₂ (Iron), AgNO₃ (Silver), etc., that are injected into the body and after attaining the desired concentration in the targeted tissue (usually tumor), these ions form nanoscale clusters and particles by utilizing the target tissue microenvironment (Scheme. 1). Similarly, various plants and microbial cells are also capable of biosynthesis of nanoscale materials and particles by using their own enzymes. These intra or extracellularly biosynthesized nanomaterials may be used for various biomedical and clinical applications. They may have higher biocompatibility and less toxicity, and enhanced surface areas. Control of particle size and shape is also possible by this method¹⁰.



Scheme 1. Mechanistic summary of the factors involved in nanoclusters biosynthesis within cancer cells and their potential biomedical applications reported so far.

Given the advantages of biosynthesizing nanoclusters from ionic precursors, the mammalian cells have been utilized for *in situ* biosynthesis of nanoscale materials for biomedical applications, especially for cancer theranostics and neurodegenerative diseases.

2. Biosynthesis

Preparations of nanoscale materials by utilizing natural biological systems are considered as green biosynthesis. The natural biosystem could be comprised of plants, bacteria, fungi, algae and eukaryotic cells, especially mammalian cells and their pathophysiology¹¹. The plant cells have been reported to have the ability to biosynthesize inorganic and organic nanoscale particles from their environment and soil concentrated with specific pre-ionic solutions. The phytochemicals which are responsible for the nanoscale materials synthesis include alkaloids, glycosides, terpenoids and phenolic compounds including tannins, coumarins, and flavonoids.¹² The biosynthesized nanoparticles obtained from phytoextracts exhibit a relatively homogenous size: For example, the silver nanoparticles from *Acalypha indica*¹³ possess a size range of 20-30 nm. The detailed plant nanoparticles biosynthesis can be followed in several recent comprehensive reviews¹⁴⁻¹⁶.

Similarly, the role of fungi and algae in green nanotechnology has been extensively investigated. The biosynthesis of nanoscale materials especially metal oxides have recently become popular. For instance, brown algae (*Bifurcaria bifurcata*) extracts have been reported with the ability to produce Copper oxide (CuO) nanoparticles (5-45 nm) from 1.0 mM copper sulfate (CuSO₄) solution¹⁷. It is well known that fungi secrete sufficient enzymes that can be used for the green production of such nanoscale materials. Recently, Vetchinkina et al. used *Lentinus edodes*, *Grifola frondosa*, *Pleurotus ostreatus* and *Ganoderma lucidum* fungi extracts to biosynthesize gold nanoparticles from HAuCl₄ solution¹⁸. The fungal extracts contained phenol oxidizing enzymes (i.e., laccases, tyrosinases, and Mn-

peroxidase), which were key players in the gold nanoparticle biosynthesis.

Different microbial species (spp.) have also been reported to synthesize nanoscale materials by using the cellular enzymes of the microbial species to convert pre-ionic solutions to nanoparticles and clusters¹⁹. These biogenic synthesized nanoparticles have higher enzymatic catalytic activity, enhanced surface area and exhibit a higher cell nanoparticle interface due to the variation of the ambient conditions, i.e., microbial intra and extra cellular pH, osmotic pressure and temperature variations²⁰. Microorganisms usually take the metal ions from their environment and with the help of enzymes convert them to the nanoscale materials. These biosynthesized nanoparticles are further classified either as intracellular (i.e., formed from metallic ions that are transported into bacteria in the presence of intracellular enzymes) or extracellular nanoparticles (i.e., metallic ions trapped on the surface of bacteria and reduced to nanoscale materials)²¹. These types of nanoscale materials include gold, silver, platinum, manganese and their associated nanocomposites.

3. In situ biosynthesis using redox-imbalanced mammalian cells

Medical bioimaging has become an indispensable tool for early, rapid, accurate and cost-effective diagnosis of cancer and many other non-cancerous diseases. In case of cancer, the diagnosis before the onset of metastasis to vital organs helps decrease the mortality rate and enhances the patient's quality of life. Although pre-synthesized nanoscale materials have been reported with promising results, there are various drawbacks of nanoscale materials, i.e., the poor target recognition, autoimmune reactions, lower serum albumin binding, the hydrophobic nature of nanoscale particles and adverse effects to vital organs^{22, 23}. Moreover, the pre-synthesized nanomaterials surface charge is also a matter of concern, e.g., the cell membrane is negatively charged and all negatively charged nanomaterials will lead to poor target recognition and prolonged

circulation time will result in adverse toxic effects. In addition, the pre-synthesized nanoparticles have to rely on the passive cellular uptake to pass the cell membrane and have to escape the endosomal/lysosomal pathway within the cell for desired theranostics effects.

To avoid these limitations, a new approach of in situ biosynthesis via mammalian cells has been introduced. In situ biosynthesis of metal nanoscale materials has been described as green chemistry, and the resulting materials are considerably more biocompatible as compared to pre-synthesized nanoscale materials. Recently, mammalian cells and certain pathophysiological conditions have been reported within in situ biosynthesis potential²⁴⁻²⁶.

3.1. Neoplastic cells

In last few years, the cancer microenvironment has been exploited to biosynthesize metallic nanoclusters. The cancer cell biology is varied from the healthy cells, thus provide a scaffold that can convert ionic solutions to nanoscale materials. In situ bio-mineralization of the inorganic salts have been extensively studied and analyzed via fluorescence spectroscopy, UV-Vis-NIR, scanning electron microscopy (SEM), transmission electron microscopy (TEM), EDS, X-ray photoelectron spectroscopy (XPS), confocal scanning microscopy and in vivo lab-animals bioimaging system for nanoparticles distribution studies and target recognition. Different metallic nanoparticles biosynthesis reported so far are as follow;

3.1.1. Gold biosynthesis

Biomedical applications of nanoscale gold materials have been exponentially increased from last few decades. These Au nanomaterials have primarily been investigated as fluorescent bioimaging probe for cancer and various non-cancer diseases. However, such nanoscale gold materials may themselves possess significant health hazards as reported by Falagan-Lotsch et al. and others; abrupt exposure to gold nanoparticles even at low doses induced significant

cytotoxic effect²⁷. Therefore, a new approach to biosynthesize gold nanoclusters with higher biocompatibility has been introduced by Wang et al.²⁸. They reported gold nanoparticle formation inside the cancer cell (hepatocellular carcinoma cells; HepG2 and myeloid leukemia cells; K562) cytoplasm around the nucleus, whereas the normal embryonic hepatocellular cells (L02), used as control were unable to biosynthesize the gold nanoclusters from a 10 $\mu\text{mol L}^{-1}$ HAuCl₄ solution. Earlier Anshup et al. reported that biomineralized gold nanoparticles within cervical cell lines (HeLa, SiHa) and human neuroblastoma (SKNSH) were formed and ranged up to 100 nm size²⁹. They suggested that ions transport takes place via the diffusion process and the relatively lower concentration with smaller size nanoparticles can be found in the nucleus. (Fig. 1) After two years, the reports of Shamsaie et al. also confirmed the Au nanoparticles formation within the cancer cells and given the credit of Au biomineralization to cell membrane sugars and enzymes³⁰.

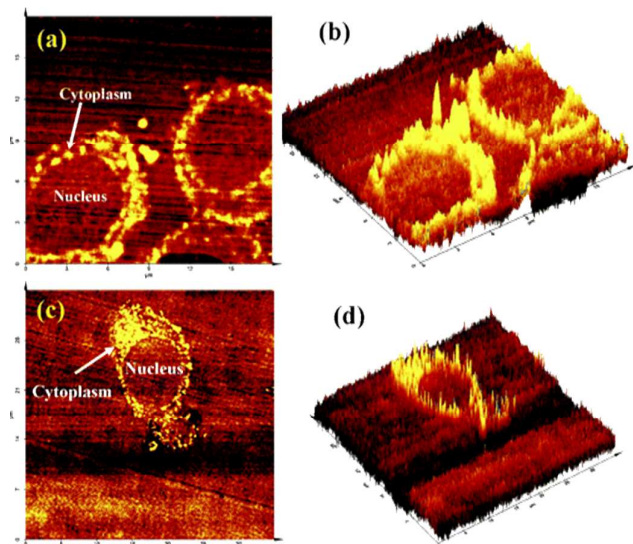


Fig. 1 Scanning near-field optical microscope images of microtomed SKNSH cells in two (a) and three dimensional (b) views, whereas (c) and (d) are HEK cells images after nanoscale Au biosynthesis. Scan area for SKNSH cells is 20 X 20 μm , whereas HEK is 35 X 35 μm . Adapted from the Ref.²⁹, Copyrights 2005 American Chemical Society.

The neoplastic tissue microenvironment is different from healthy tissue homeostasis due to increased H₂O₂ production resulting in an elevated reactive oxygen species (ROS) level³¹. In the tumor cells, dioxygen reduction leads to the generation of ROS that subsequently provides an extra electron to the pre-ionic solution, leading to nanoscale biomineralization. Also, it has been reported that the initial nanoparticles formation is close to the cell membrane, the area which is enriched with the enzymatic pool, especially NO-synthases and NAD(P)H-oxidases³². The studies of El-Said et al. have also demonstrated that NADP and QOH-1 enzymes are having a contribution to the formation of Au nanoparticles from Au⁺³³³. Husseiny et al. suggested that the gold metal ions can easily cross the cell membrane and act as electron acceptor inside the cytoplasm and mitochondria³⁴, whereby they can disturb any specific electron transport pathways and result in nanoparticles formation. Since the mitochondria are well distributed within the cytoplasm, the biosynthesized nanoparticles were likewise distributed and equally found within the cytoplasm (Fig. 2).

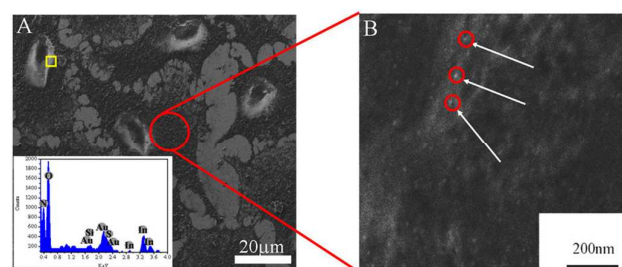


Fig. 2 Gold nanoclusters in situ biosynthesis within the neoplastic tissue. (A) Scanning Electron Micrograph (SEM) of HepG2 cells after incubation with HAuCl₄ 10 $\mu\text{mol/L}$ solution and EDS as inset, whereas (B) is an enlarged image showing gold nanoclusters denoted by white arrows. Adapted from Ref.²⁸, Copyrights 2013, Macmillan publishers.

Recently, the peptides secreted by human breast adenocarcinoma cells (MCF-7) in response to gold salt exposure were regarded as a biological factor for anisotropic gold nanoparticles formation³⁵. It has been suggested that sudden exposure of cells to gold salt will result in lowering of pH that will denature the cell membrane and serum proteins, which in turn will reduce the Au³⁺ to Au⁰ gold nanoparticles. Moreover, the cells in stress condition also secrete peptides that bind to specific facet resulting in anisotropic gold nanoparticles formation. As a whole, this study suggests that peptides secreted by the cancer cells to the surrounding microenvironment and cell membrane protein biomineralize the gold salt to nanoparticles. Contrary to these findings, Kunoh et al., reported that genetic materials from the nucleus are responsible for Au³⁺ reduction to Au⁰. They reported that of various nucleosides and nucleobases only guanine and guanosine are potential reductants for Au nanoparticles formation³⁶. Since the biological system is complex with multiple factors and molecules regulating each other simultaneously, therefore on the bases of currently available data it's hard to credit only one factor as sole reducing agent for gold nanoscale biomineralization. Moreover, the various cell growth media and factors have also been reported with the effect on the size and shape of biosynthesized gold and other metallic nanoparticles.³⁷

Similarly, Lai et al. reported gold nanoclusters biosynthesis for bioimaging of Alzheimer disease (AD)³⁸. As is the case with cancer cells, the ROS level is elevated in Alzheimer patients' cerebral tissue due to an active exchange of various redox metal ions^{39,40}. The AuCl₄⁻ ions were accumulated in the hippocampus of mice models, which is the first and most seriously affected part of a brain in the AD. After accumulation of gold ions in the brain, they rapidly start forming gold nanoclusters, which were then used as nanoprobe for the CT and fluorescent bioimaging of the AD brain. (Fig. 3) Besides, the findings of Chatteraj et al. proved Au nanoclusters formation within the human lung cancer cell line A549. They observed 20-40 times higher fluorescence intensity within cancer cells as compared

to normal cells with about 1-3 nanoseconds lifetime within cells. The size of nanoclusters was ~2 nm and Au nanoclusters at this size range exhibit excellent fluorescent properties⁴¹.

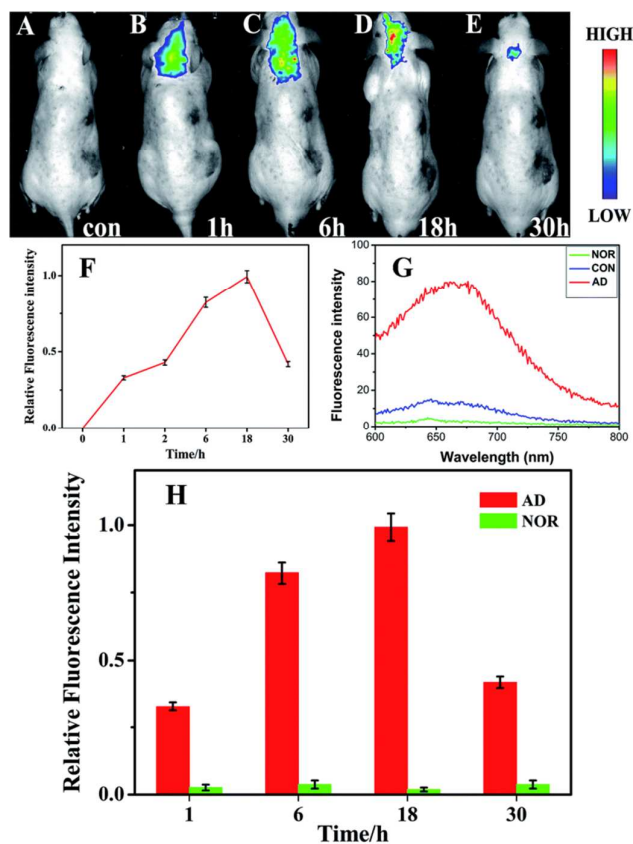


Fig. 3 Fluorescence bioimaging of Alzheimer Disease via in situ biosynthesized gold nanoclusters. Neurodegenerative diseases murine model is exhibiting fluorescence at different time intervals, i.e. 1 hour (B), 6 hours (C), 18 hours (D) and 30 hours (E), after injection of 10 mmol/L HAuCl₄ solution, whereas (A) control without injection. (F) is relative fluorescence intensity and (G) is the fluorescence intensity, whereas (H) is comparative fluorescence intensity of control with treated models at various time intervals. Adapted from the Ref. ³⁸, Copyrights 2016, Royal Society of Chemistry.

3.1.2. Silver Nanoparticle biosynthesis

Biosynthesized silver nanoparticles obtained via plant extracts, or microorganisms biosynthesis are the most abundantly investigated nanoparticles for biomedical applications. Recently, Gao et al. exploited the potential of cancer cell microenvironment to form silver nanoparticles from the AgNO_3 solution combined with glutathione (GSH), i.e. $[\text{Ag}(\text{GSH})]^{+42}$. Both ex vivo and in vivo experiments confirmed rapid biosynthesis of Ag nanoparticles when Ag ions conjugated with GSH. They bioimaged trace amount of cervical cancer cells (HeLa) within the xenograft animal model in vivo, and also in vitro by using Near Infrared (NIR) emission for photoactivation (excitation 590, emission 670 nm) of the clusters formed within the cell. The NIR experiment has the advantage of deeper penetration (2-3 cm) within living tissue and is according to WHO recommendations (i.e., 600-1000 nm, as the maximum transparency of human skin is centered on 800 nm). (Fig. 4)

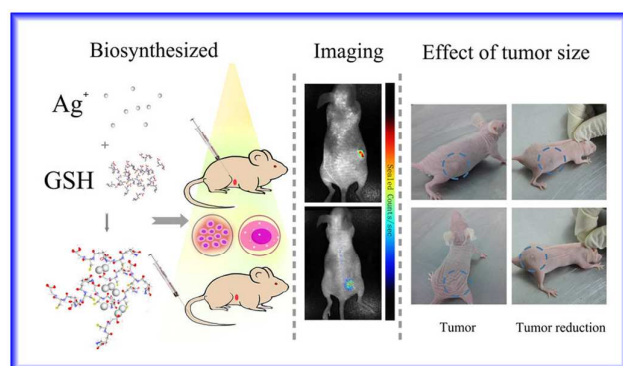


Fig. 4 Fluorescence bioimaging of murine xenograft models after Silver nanoclusters formation within tumor tissues and cell cultures (HeLa). The pre-ionic solution of $\text{Ag}[\text{GSH}]^+$ was injected to biosynthesize Ag nanocluster in situ, exhibiting excellent theranostics effect via tumor fluorescence bioimaging and regression. Adapted from the Ref. ⁴², Copyrights 2014 Macmillan Publishers Ltd.

GSH is a thiolated tripeptide present in normal eukaryotic cells (ca 5 mM) responsible for the maintenance of cellular redox homeostasis by oxidation to glutathione disulfide (GSSG). It has been shown that cancer cells are higher in GSH-GSSG concentration as compared to normal cells⁴³. The higher concentration of GSSG within neoplastic tissue and cells may be attributed to the higher generation of ROS and RNS. Meanwhile, the disulfides and thiols possess a higher affinity towards silver ions which helps to promote monolayer self-aggregation. Therefore, the glutathione complexation and silver ions reduction assist in Ag nanoclusters formation, which may lead to a new route for selective bio-marking of cancer cells via fluorescence bioimaging.

The recent findings of El-Said et al. showed successful Ag and Au nanoparticles formation from their respective salts within cancer cells (HeLa, MCF-7)³³. The

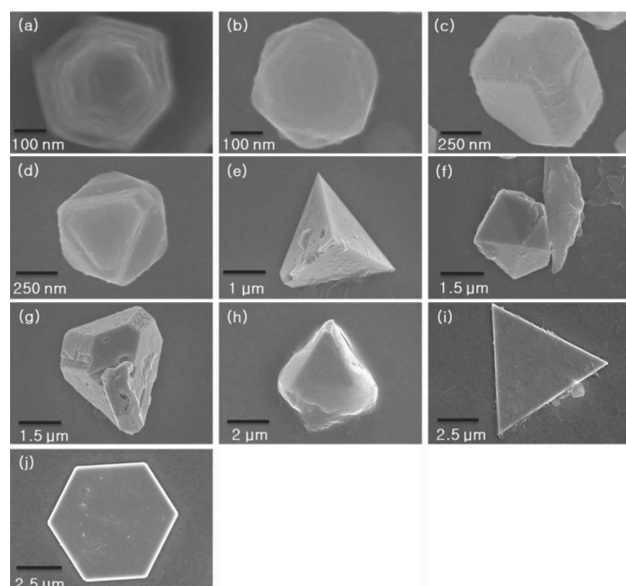


Fig. 5 Scanning Electron Microscopic images of biosynthesized gold nanoparticles after HeLa cells incubation with HAuCl_4 solution for 4 (a,b), 08 (c,d), 14 (e,f), 21 (g,h) and 28 days (I,j). Adapted from Ref. ³³, Copyrights 2013 Willey-VCH Verlag GmbH & Co. KGaA, Weinheim.

intracellular biosynthesized nanoparticles were used for Surface Enhanced Raman Spectroscopy (SERS). Their study reveals that cell membrane and extracellular secreted proteins can be utilized for nanoscale particles synthesis, whereas whole cell incubation (up to 28 days) with respective ionic solution results in microscale particles formation.

The microscale particles may result from the biosynthesized nanoparticles that upon secretion to surrounding environment aggregated and formed microparticles. The intracellular enzymes present either in the cell nucleus or nuclear membrane or cells membrane may be responsible for the nanoparticles formation. As per their report, the whole cell lysate or nuclear lysate could form the nanoparticles in several minutes whereas the cytoplasmic content may take several hours for the nanoparticles formation. (Fig. 5)

3.1.3. Rare Earth metals biosynthesis

Compared to other organic and inorganic (metallic) counterparts, Rare Earth Ions (REI) also have significant potential to form fluorescent nanoprobe via in situ biosynthesis. These ions have narrow emission lines and a wide band gap between excitation and emission wavelengths⁴⁴. They may not only be used as fluorescent probes, but they may also be able to influence cellular functionalities, i.e., their concentration will define cell apoptotic or proliferative, anti or pro-oxidant properties⁴⁵. The REI has empty f and d orbitals, which makes them excellent fluorescent probes to detect tumor cells at minute quantity via bioimaging. REI or lanthanide ions generally have weak fluorescence properties in aqueous solution due to low molar absorptivity and low fluorescence quantum yield⁴⁶. However, some reports have suggested their conjugation with a proper ligand can increase the fluorescence intensity⁴⁷.

Europium (Eu) is also a member of REI or lanthanide group. Recently, Ye et al. biosynthesized a Eu complex by exploiting the tumor cell environment and then used the resulting material as a fluorescent nanoprobe for the detection of cervical cancer (HeLa)⁴⁸. They

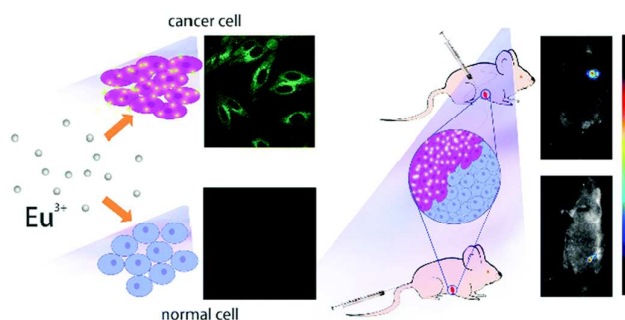


Fig. 6 Tumor bioimaging via Europium biosynthesized nanoclusters. The hepatocellular carcinoma culture and murine model exhibited fluorescence within 24-48 hours. Eu nanoclusters formation after incubation/injection of 0.01 mmol/L $\text{Eu}(\text{NO}_3)_3$ solution to cells and animal models. (Excitation wavelength was 488 nm). Adapted from Ref ⁴⁸, Copyrights 2016 Royal Society of Chemistry.

incubated cancer cells in 0.01 mM $\text{Eu}(\text{NO}_3)_3$ solution for 24-48 hours, and after employing the freeze-thaw method, the nanoscale Eu material was isolated from the cells. These nanoclusters were characterized by confocal bioimaging and EDS within the cells, while TEM and X-ray photoelectron spectroscopy (XPS) was used to determine the particle size and valence state of the europium atoms. They observed mixed valence state of Eu (i.e., III and II), which can be attributed to the tumor microenvironment that reduced Eu (III) and allowed Eu (II) to form within the cells. Similar to other nanoprobe biosynthesized in situ, the formation of the Eu complex was also favored by the elevated level of H_2O_2 and NADPH- dependent GSH within the cancer cells that allowed Eu (III) to form the Eu complex. Earlier studies reported that the Cerium(III)-GSH complex could be synthesized in vitro by using the redox conditions for Cerium (III) and GSH⁴⁹, and it is likely that Eu undergoes the same reaction under these conditions. Meanwhile, the proteomic studies of cancer cells treated with Eu (III) also suggested the involvement of p53 and NADP(H)-oxidase in the neutralization of the antioxidant pathways and persistent fluorescence up to 48 hours (Fig. 6).

3.1.4. Zn nanoclusters biosynthesis Zinc (Zn) is a most important precursor for many enzymes, immune regulatory system, and cellular functionality⁵⁰. Zn was the first metal ion which was detected by biosensors in the human plasma by Mahanand and Houck in 1968⁵¹. Zinc and Copper ions are the most investigated and well-defined metal ions maladies associated with homeostasis⁵². Both ZnCl₂ and Zn(C₆H₁₁O₇)₂ (Zn Gluconate) have been reported to be able to form nanoclusters within living cells. A lower Zn concentration has been reported in various ailments including neoplasms, especially prostate cancer⁵³. Also, the interaction of Zn ions with glucose and oxygen leads to increased ROS and RNS generation compared to normal tissues^{54,55}.

Given these properties, Su et al. biosynthesized Zn nanoclusters from a Zn Gluconate (0.08 mM) solution within neoplastic cells cultures, both in vitro and in vivo in xenograft models⁵⁶. Pre-synthesized nanoscale Zn has already been reported to exhibit fluorescent properties⁵⁷. Indeed, the biosynthesized Zn nanoclusters reported by Su and coworkers were successfully used for bioimaging of HeLa and HepG2 cancer cells. Again, the specific microenvironment of these cancer cells was essential for the nanocluster formation.

Recently, Du et al. combined Zn with Fe ions to biosynthesize a cancer multimode bioimaging probe from a single pre-ionic solution⁵⁸. They used 300 μM Zinc gluconate and 300 μM FeCl₂ to biosynthesize nanoclusters in various cancer cell lines including HePG2, HeLa, U87 (glioblastoma) and L02 as control, both in vitro and in vivo. The Zn nanoclusters were found to be highly biocompatible. They exhibited fluorescence both in the cancer cells cultures and tumors in xenograft animals. (Fig. 7)

The pathophysiology of neurodegenerative diseases has also been associated with an imbalance of ion concentrations of Zn, Cu, and Fe. These ions modulate molecular aggregation of certain proteins associated

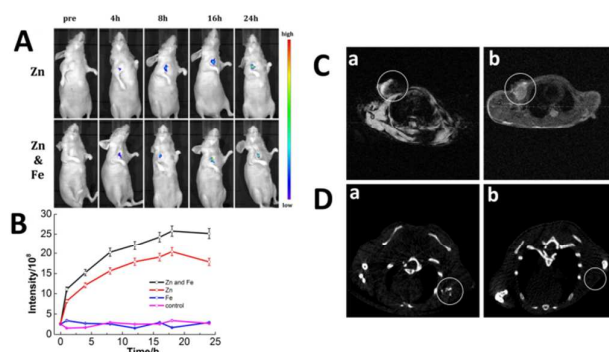


Fig. 7 Fluorescence, CT and MRI multimode bioimaging achieved via Zn and Fe nanoclusters biosynthesis within xenograft tumor models. The hepatocellular carcinoma tumor models with fluorescence (A), MRI (C) and CT (D) bioimages, neoplastic tissue denoted by white circles, whereas (a) is 5 mM FeCl₂ and Zn Gluconate treated models and (b) is controlled. Similarly, (B) is showing fluorescence intensity of various treated murine models. Adapted from Ref⁵⁸, Copyrights 2017 Tsinghua University Press and Springer-Verlag Berlin Heidelberg.

with the neurodegenerative disease. Therefore, injection of Zn ions may help both in remediation of the imbalance and also make possible bioimaging of various cerebral diseases. Recently, Lai et al. successfully bioimaged AD with Zn Gluconate by forming nanoclusters inside the brain of murine models⁵⁹. Similarly, cerebral stroke, which is not a primary brain disease, but occurs due to the compromised blood supply to certain parts of the brain, was successfully bioimaged by Zhao et al.⁶⁰ They claimed hypoxic conditions and inflammation as a primary cause for the formation of Zinc nanoclusters from Zn Gluconate solution.

More recently, Wu et al. reported ZnO nanoclusters spontaneous formation within the mammalian copulatory blood. Furthermore, they claimed that serum albumin were the key ingredients to biosynthesize the ZnO nanoclusters from Zn gluconate rather than glutathione or metallothionein. They also proposed that Zn ions above the physiological level are converted to ZnO nanoclusters by the serum albumins

and then safely excreted from the body⁶¹. All the aforementioned reports confirm the ZnO nanoclusters in situ biosynthesis and potential biomedical applications in theranostics; nevertheless, the exact mechanism of ZnO nanoclusters biosynthesis still remains unknown.

3.1.5. Nano Fe in situ biosynthesis

Iron has been reported as a contrast agent in diagnostic bioimaging via X-ray computed tomography (CT) and magnetic resonance imaging (MRI). The MRI ensures deep penetration whereas CT reveals the anatomical structure of the target tissue. MRI contrast agents have been classified as T1 and T2 agents, depending on their resonance properties. Fe₃O₄ can be classified as a T2 imaging agent for clinical applications due to its transverse relaxation time in H₂O⁶². Various pre-synthesized nanoscale Fe based materials include Fe₃O₄⁶³, FeNPs⁶⁴, CoFe₂O₄⁶⁵, NiFe₂O₄⁶⁶, Au-Fe₃O₄⁶⁷, Au-FePt⁶⁸, and MnFe₃O₄⁶⁹ etc. Similar to other pre-synthesized nanoscale materials, iron also has some adverse effects including cellular leakage, impaired mitochondria function, DNA damage, chromosome condensation and inflammation⁷⁰.

Recently Zhao et al. used a new approach to synthesize iron nanoclusters by utilizing the cancer microenvironment⁷¹. They combined 10 mmol L⁻¹ FeCl₂ and 5 mmol L⁻¹ HAuCl₄ solutions to form iron and gold nanoclusters for multimode cancer bioimaging. They exploited the potential of the cancer microenvironment to convert the pre-ionic solutions (Fe²⁺) to Fe₂O₃ and AuCl₄⁻ to gold nanocomposites via HeLa, HepG2 and U87 cancer cell lines and also in xenograft models as well (Fig. 8). Meanwhile, the biocompatibility of the Iron and gold nanoprobe was evaluated via MTT assay and vital organ (Liver, Kidney, and Spleen) functionality by histopathology and serum biomarkers. All of the in vivo and in vitro biocompatibility trials proved the inertness of the biosynthesized Au-Fe nanoprobe to vital organs indicating the relative lack of toxicity of these materials in biomedical applications.

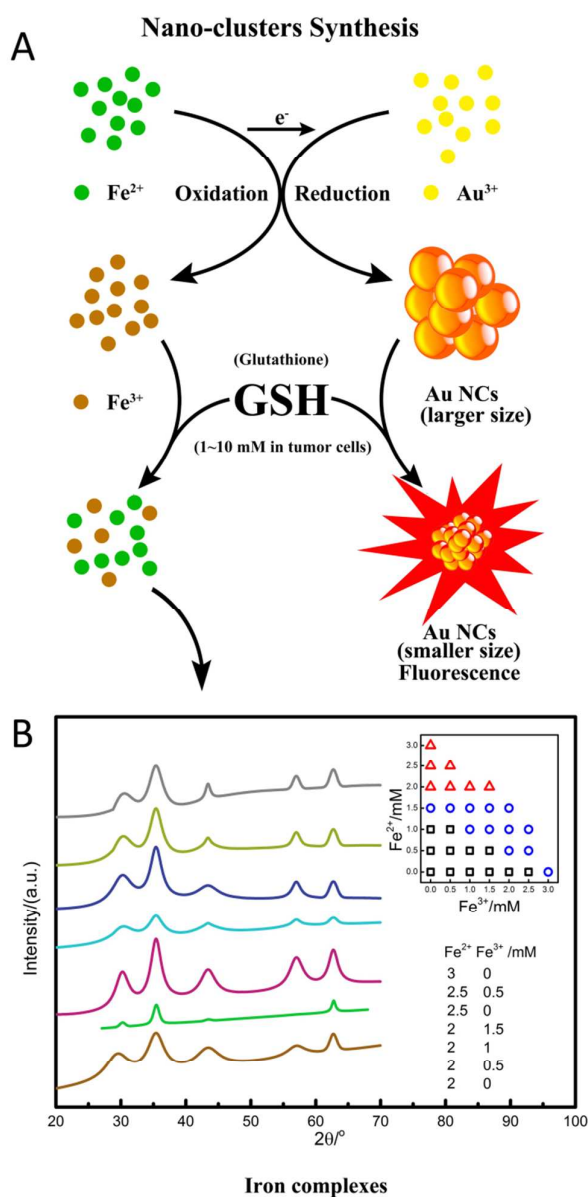


Fig. 8 (A) Mechanism of Iron and Gold nanoclusters biosynthesis within the cancer cells and (B) is the XRD pattern of Fe complexes. Adapted from Ref. ⁷¹, Copyrights 2016 Willey-VCH Verlag GmbH & Co. KGaA, Weinheim.

The neoplastic microenvironment is somewhat different from normal tissues due to the higher amount of nicotinamide adenosine dinucleotide phosphate hydrogenase enzyme (NAD(P)H), glutathione (GSH-GSSG), as well as RNS and ROS, and lower pH value. The

lower pH value may be attributed to lack of blood vessels, higher metabolic rate, and decreased oxygen concentration. All these factors play a pivotal role in the formation of fluorescent, and magnetic nanoclusters from a simple ionic solution injected into the body. Since the GSH-GSSG is 1-10 times higher in the cancer cells as compared to normal healthy tissues, the Fe^{2+} ions are oxidized to Fe^{3+} ions which assist in gold nanocluster formation. Meanwhile, the GSH-GSSG control the Fe^{2+} and Fe^{3+} ratio and additionally form iron nanoclusters and reduce gold nanoclusters size ultimately leading to efficient fluorescence probes (Fig. 9).

Similarly, Du et al. used Fe ions (Fe^{2+}) combined with Zn (Zn^{2+}) to achieve cancer multimode bioimaging via fluorescence (Zn nanoclusters) and CT, MRI

(paramagnetic Fe_3O_4 nanoclusters) as discussed earlier⁵⁸ (Fig. 10). Another study by the same group (Du et al.) used Zeolitic Imidazole Framework-8 (ZIF) to adsorb Fe ions and successfully deliver Fe ions to target tissue, i.e., the tumor, both in vitro and in vivo⁷². After accumulation in neoplastic tissue, the ZIF was biologically degraded to form ZnO nanoclusters, whereas Fe ions were converted to paramagnetic Fe_3O_4 nanoclusters triggered by the combination of lower pH (elevated acidity), oxygen (higher ROS level) and an elevated level of GSH-GSSG in the neoplastic environment.

3.1.6. Pt nanoclusters biosynthesis

Platinum is well-known for its photothermal properties. In the biomedical realm, its potential has long been used for chemotherapeutic anti-cancer drugs, e.g., Cisplatin, Carboplatin, Oxaliplatin, etc.⁷³ In spite of the fact that these drugs have been in use for many years, their exact mode of action still is under investigation. Their potential cytotoxic effects are significant; for instance, Pt adducts with pyridine ligation have been attributed to cytotoxic effects. Similarly, conjugation with tRNA has potential cytotoxicity⁷⁴. Also, the octahedral Pt(IV) state has been reported to cause gastrointestinal and blood adverse effects after oral administration⁷⁵. In tumor bioimaging, the role of nanoscale Pt has been limited compared to its use in chemotherapeutic agents. Problems with the use of Pt in bioimaging include poor photostability, rapid photobleaching, and self-aggregation⁷⁶. Moreover, the well-known Pt anticancer drug cisplatin (cis-diamminedichloroplatinum II) and similar derivatives are well known to cause severe nephrotoxic effects^{77,78}. Indeed, the new biosynthetic approach has the potential to overcome these limitations as Chen et al.⁷⁹ did not observe any adverse effects after nanocluster formation with cisplatin; however further studies may whether this is generally the case beyond this specific example may well be required. The hypoxic reducing environment can be utilized to in situ biosynthesize Pt nanoclusters from their ionic precursor solutions.

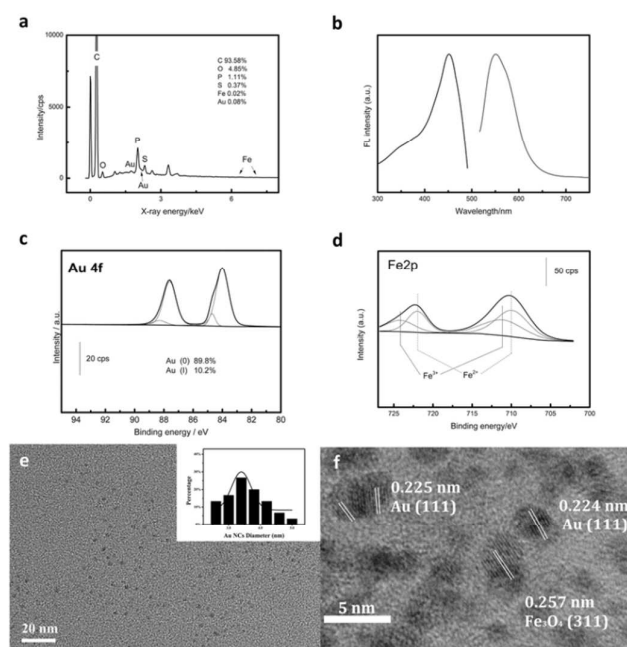


Fig. 9 Characterization of biosynthesized Fe and Ag nanoclusters within the neoplastic tissue. TEM (e,f) EDS (a), Fluorescence spectrum and XPS of cellular (c) and tumor extracts (d) confirming the co-existence of Fe^{2+} and Fe^{3+} ions at 09-01 ratio, respectively. Adapted from Ref. ⁷¹, 2016 Copyrights Willey-VCH Verlag GmbH & Co. KGaA, Weinheim.

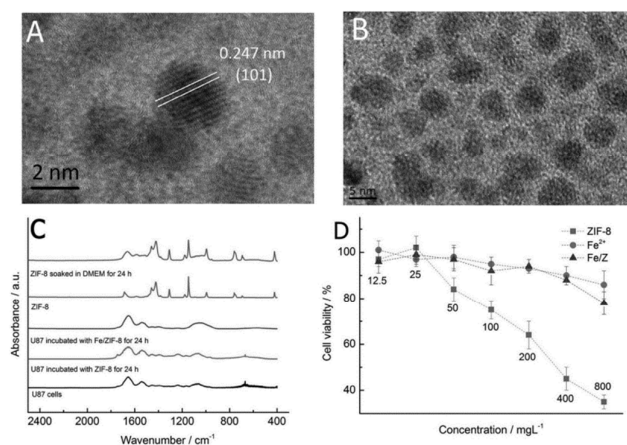


Fig. 10 Tumor tissue in situ biosynthesized nanoclusters characterization. (A) is the TEM image of in situ biosynthesized ZnO nanoclusters, (B) is the mixture of ZnO and Fe₃O₄ nanoclusters, whereas (C) is the FTIR spectra of glioblastoma cells, ZIF-8 and their mixtures. (D) is the MTT assay for cell viability after treatment. Adapted from the Ref.⁷² Copyrights 2017 Willey-VCH Verlag GmbH & Co. KGaA, Weinheim.

Recently Chen et al. used 5 mmol L⁻¹ Chloroplatinic acid (H₂PtCl₆) solution to biosynthesize Pt nanoclusters by using various cancer cell lines including HeLa, HepG2, and A549 (lung cancer)⁷⁹. For the theranostics effect, they combined Tetra sulphonatophenyl porphyrin (TSPP) with spontaneously formed round shaped 3.3 nm Pt nanoclusters. The TSPP was used to enhance the fluorescence by a synergistic effect that realized the photothermal effect of Pt nanoclusters⁸⁰. The elevated level of GSH-GSSG was again responsible for chemical etching of Pt sols (Fig. 11).

3.2. Normal cells and Biosystems

Apart from exploiting the tumor microenvironment, some normal body cells and their microenvironment have also been reported to have the potential for nanoscale materials biosynthesis. Larios-Rodriguez et al. reported epithelial cells with the potential to biosynthesize gold nanoparticles (average size 49 nm)⁸¹. They deposited 10 μl of 0.1 M tetracholoauric acid solution on the finger of a subject individual resulting immediately in a pale color. This color turned purple

after three hours at room temperature, indicating nanoscale gold formation. The skin (epithelium) was then removed and was further investigated under TEM for nanoparticles characterization. They proposed that certain enzymes and sugars may be responsible for reducing Au (III) ions to Au (0), which further aggregated into gold nanoparticles. However, the actual mechanism within non-neoplastic cells is still unknown.

Recently, the US army research labs have also demonstrated in their report that NG108-15 neuroblastoma-glioma hybrid cells when exposed to the H₂AuCl₄ solution, within 24 hours of gold nanoclusters were formed. They proposed its potential use in detection of the brain trauma⁸². Meanwhile, West et al. also reported neuronal microglial cells (C8B4) with the potential of Au nanoclusters formation ability. They claimed that glutamate was a key player in the Au nanocluster formation rather than the elevated level of ROS as most researchers claimed for the neoplastic cells.⁸³

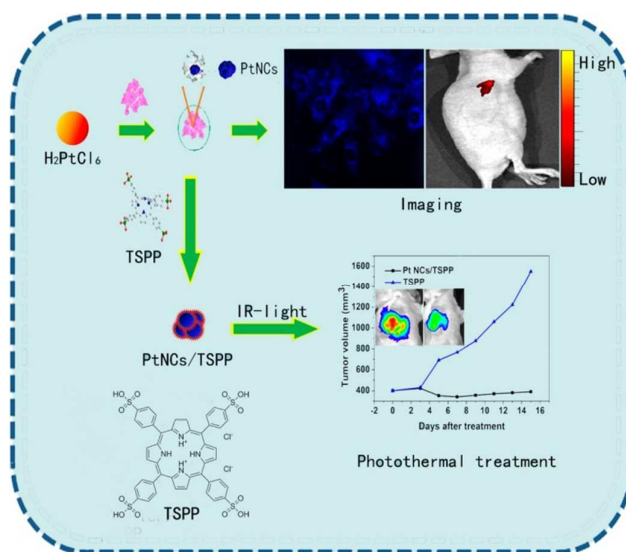


Fig. 11 Pt Nanoclusters in situ biosynthesis inside the cancer cells and tissues after inoculation /injection of H₂PtCl₆ and TSPP, and their further theranostics effect. Adapted from Ref.⁷⁹, Copyrights 2015 American Chemical Society.

The formation of Au nanoclusters in non-neoplastic cells and microenvironment are of great interest, especially in the neuroscience, to help in understanding the neural functionality or ailment.

Most recently, human adipose mesenchymal stem cells (MSC) were used to biosynthesize magnetic nanoparticles by transfecting the MSC by bacterial magnetotactic gene, i.e., *mms6*⁸⁴. After inoculation of 34 mM ferric quinate solution, the cells began to synthesize magnetic nanoparticles (Fe_3O_4) without affecting cellular activities, such as multiplication and differentiation. (Fig. 12)

Another approach towards exploiting the neoplastic environment for cancer therapeutics was reported by Mackay et al.⁸⁵ They prepared chimeric polypeptides conjugated with doxorubicin that self-assembled into particles of less than 100 nm size. These polypeptides

were then conjugated with chemotherapeutic agents and were then successfully used to deliver the Dox to target neoplastic tissue and subsequently induced apoptosis in the colon carcinoma cells (C26) and murine xenograft models. This method can be applied further to many drug delivery and bioimaging systems for cancer theranostics.

In addition to mammalian cells other in vivo experimental models have also been used to produce nanoscale materials. For instance, Earthworms have been used in various traditional Chinese medicines due to their bactericidal, cytotoxic, agglutinating, proteolytic, hemolytic and mutagenic properties⁸⁶. And recently, their potential for nanoscale materials green synthesis has been explored by Jagannathan et al⁸⁷. They prepared exudate from earthworm (*Eudrilus eugeniae*) minced tissues and treated them with 1 mM AgNO_3 solution to biosynthesize silver nanoparticles.

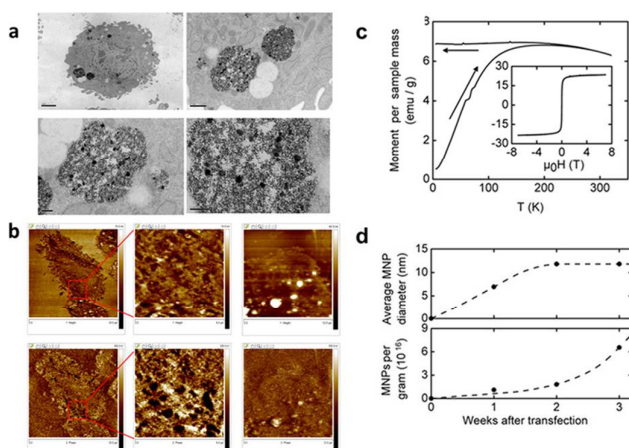


Fig. 12 Mesenchymal stem cells magnetic nanoparticles biosynthesis after magnetotactic gene *mms6* transduction from bacterial cells. (a) is the TEM micrograph, (b) is the AFM micrograph upper row and middle, whereas the lower row is the MEM images and the right column is control. (c) is SQUID magnetometry and (d) is a superparamagnetic sample (upper panel) and the dry sample (lower panel). Adapted from Ref.⁸⁴, Copyrights 2017 Macmillan publisher limited.

3.3. Biomedical applications

The nanoscale metallic biomaterials are used widely in biomedical applications including gene delivery, chemotherapeutics, anti-bacterial, antiprotozoal, diagnostics, molecule detection, bioimaging, DNA/RNA analysis and biosensors. The recent biomedical applications of nanoscale materials are based on nanomaterials prepared by traditional methods in the lab. The biosynthesized metallic nanoscale particles and clusters are still in the developing phase. Although the methodology of using mammalian cells as a scaffold for in situ biosynthesis is only a few years old, it may nevertheless lead to significant applications in the biomedical realm in the relatively near future. A few major biomedical applications developed in the last few years are summarized as follows;

3.4. Cancer Therapeutics

Silver nanoparticles synthesized from the *Melia dubia* plant extracts were reported for their anticancer effect by Kathiravan et al⁸⁸. Meanwhile, the earthworm extract based silver nanoparticles were also reported to

possess anticancer effects against hepatocellular carcinoma cells, i.e., HepG2⁸⁷. Similarly, Muthukumar and coworkers used extracts of *Carica papaya* and *Catharanthus roseus* plants to biosynthesize round shaped gold nanoparticles with potential anticancer applications against HepG2 tumor cells⁸⁹.

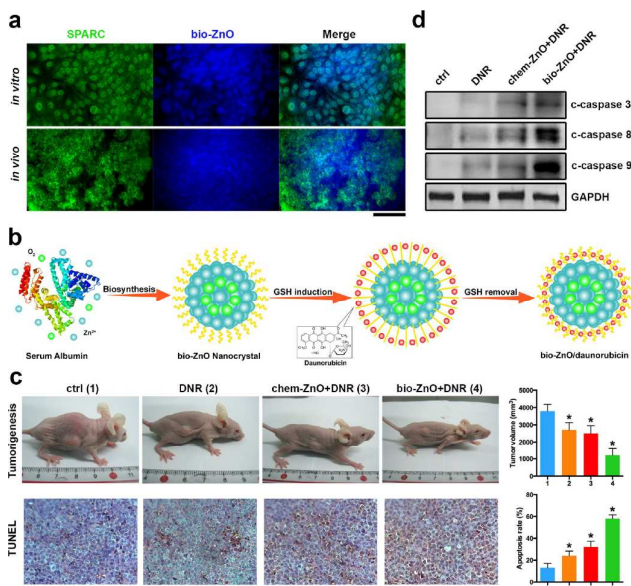


Fig. 13 Application of DNR-loaded bio-ZnO NCs to tumor growth suppression in vivo. (a) HepG2 cells were treated with 10 mg/L bio-ZnO NCs (blue) for 2 h and then stained with Alexa 488-conjugated anti-SPARC antibody (green). Scale bar: 100 μm . (b) Scheme of the synthesis of DNR-loaded bio-ZnO NCs. (c) K562 xenograft nude mice were treated (1) without or with (2) 3.2 mg/kg DNR (equivalent to the 32% loading rate on the bio-ZnO NCs), (3) 10 mg/kg DNR-loaded chem-ZnO NCs, or (4) 10 mg/kg DNR-loaded bio-ZnO NCs. The apoptotic cells were assayed by TUNEL staining. The nuclei of apoptotic cells (brown) and viable cells (blue) were stained. Scale bar: 100 μm . The bars in the histogram represent the results from five independent experiments. *Significant difference compared with the untreated group ($P < 0.05$). (d) The protein levels of cleaved caspase-3, -8, and -9 in tumor samples were analyzed by Western blot. GAPDH was detected as an internal standard. Adapted from Ref.⁶¹, Copyrights 2017 American Chemical Society.

Recently, CuO nanoparticles synthesized from leaf extracts of *Ficus religiosa* plant were reported to treat lung cancer after finding their anticancer effect on A549 human lung cancer cells⁹⁰. Similarly, biosynthesized terbium oxide (Tb_2O_3) nanoparticles by *Fusarium oxysporum* (fungus) were reported to exhibit anticancer activity against osteosarcoma cells lines, i.e., Saos-2, MG-63⁹¹. Meanwhile, the in situ biosynthesized ZnO nanoclusters were combined with DOX to bioimage and ablate the k562 tumor in murine xenograft models⁶¹. (Fig. 13)

The aforementioned in situ biosynthesized nanoscale materials involving Pt, Au, and Ag ions can also be used to induce apoptosis or necrosis in local cancer tissue during the nanoclusters biosynthesis. After photoactivation or in combination with other photosensitizers such as TSPP these nanoclusters can generate ROS (O_2^- , $\bullet\text{OH}$, $^1\text{O}_2$, and H_2O_2) and RNS that may interfere with cellular signal pathways and alter the membrane permeability to induce apoptosis or necrosis in cancer cells⁹²⁻⁹⁵.

3.5. Bioimaging agents

The history of bioimaging can be traced back to 1958 when Joseph von Gerlach stained brain cells nuclei by carmine⁹⁶. Subsequently, the discovery of Hematoxylin and Eosin led to a revolution in the histopathology of various diseases, and these two agents are still the most abundantly used worldwide, due to their low cost and reliable stain for cellular studies⁹⁷⁻⁹⁹. However, H&E satin applications are limited to fixed tissue samples only in the cytoplasm and nucleus. Therefore various other stains are used to bioimage living cells, i.e., DAPI, Hoechst, SYTO, and DRAQ. Several recent reviews have been published on these stains¹⁰⁰⁻¹⁰².

Modern diagnostics largely relies on the optical imaging of cellular organelles, DNA, RNA and other functional molecules. Currently, various bioimaging molecular probes are employed to serve this purpose. However, these probes have certain limitations including photobleaching, the poor target recognition, hydrophobicity, autoimmune reactions, and high

cytotoxicity^{103, 104}. Nanoscale materials may overcome some of these drawbacks. Most of the nanoscale materials, e.g., quantum dots (QDs) and clusters have been reported as efficient bioimaging probes for PET, MRI, CT, FRET, and fluorescence, due to their stability to photobleaching and efficient targeting ability¹⁰⁵. Among the various nanoparticles, Gold has been extensively investigated as a fluorescent and CT bioimaging nanoprobe. The nanoscale probes have been used to bioimage almost all types of cancer cell lines, inflammatory diseases, autoimmune diseases such as rheumatoid arthritis, and neurodegenerative diseases. Recently, Lai et al.³⁸ successfully investigated murine models of Alzheimer disease (AD) by using in situ biosynthesized gold nanoprobe as bioimaging tools. They found that after injecting the AD models with HAuCl_4 ionic salts, within two hours the hippocampus region of the AD model brain become fluorescent as compared to the normal control. Similarly, the work of Wang et al. demonstrated bioimaging of cancer via in situ biosynthesized nanoclusters²⁸. In addition to gold, Zn nanoclusters have also been used to bioimage cerebral ischemic stroke⁶⁰ and Alzheimer's disease³⁸, whereas Pt nanoclusters were reported to exhibit cancer theranostics properties⁷⁹. Most of the in situ biosynthesized nanoprobe were primarily used to diagnose cancer and neurodegenerative maladies, followed by therapeutics and drug delivery systems.

3.6. Antimicrobials

The anti-microbial effect of nanoscale materials has become popular in recent years due to both lower cost and enhanced efficacy against drug-resistant microbes. The most common microorganisms including drug-resistant bacterial strains, i.e., *Klebsiella pneumoniae*, *Escherichia coli*, *Pseudomonas aeruginosa* have been reported to be quite sensitive to nanoscale materials¹⁰⁶. Most of the nanoscale materials generate reactive oxygen and nitrogen species including superoxide, $\bullet\text{OH}$, H_2O_2 , and $\text{NO}\bullet$, which react with cellular organelles, genetic materials (DNA, RNA) and the cell wall to induce apoptosis or necrosis within the cell. They may

also interfere with cellular signal pathways resulting in altered cellular activities and functionality¹⁰⁷. Similarly, non-ROS, RNS generating nanoparticles, e.g., nano silver generate silver ions that interfere with functional proteins and enzymes, disrupt cell membranes, and deactivate the respiratory chain and DNA replication¹⁰⁸.

Recently, Shinde et al. used Guava leaves extract to produce nanoparticles. They also reported on the antimicrobial effect of their nanoparticles¹⁰⁹. Also, Mariselvam et al. used *Cocos nucifera* phytoextracts, i.e., ethyl acetate and methanol to synthesize silver nanoparticles against the clinically most significant pathogenic bacteria including *Pseudomonas aeruginosa*, *Klebsiella pneumoniae*, *Bacillus subtilis* and *Salmonella paratyphi*¹². Similarly, the CuO nanoparticles biosynthesized by the *Gloriosa superba* L. plant extracts had excellent bactericidal effects against Gram-negative (i.e., *Klebsiella aerogenes*, *E. coli*, *Pseudomonas desmolyticum*) and Gram-positive (i.e., *S. aureus*) pathogenic bacteria. The gold and silver nanoparticles synthesized from the ginger extracts have also been reported to show antibacterial effects against gram-positive (*Staphylococcus* and *Bacillus* spp.) and gram-negative (*Klebsiella* spp.) bacteria¹¹⁰.

Meanwhile, the silver nanoparticles synthesized from earthworm exudates were reported to possess excellent antibacterial effects against *Proteus vulgaris*, *Klebsiella pneumoniae*, *E.coli*, *Bacillus subtilis* and *Bacillus thuringiensis*⁸⁷. Likewise, nanoparticles by Goa et al. which were biosynthesized from the mammalian cells as described earlier were excellent antimicrobials in burn wounds healing.

3.7. Fungicidal

Silver nanoparticles prepared from the earthworm exudates were evaluated for their fungicidal effects on *Candida albicans*, *Fusarium solani* and *Aspergillus niger*⁸⁷. Moreover, silver nanoparticles obtained from *Bacillus* spp. were reported with efficient fungicidal effect against *Fusarium oxysporum* when used at a concentration of 8 $\mu\text{g}/\text{ml}$.¹¹¹ Similarly, the silver nanoparticles were reported to be effective against

Trichoderma spp, Aspergillus niger, and Mucor spp¹¹². Several studies have been reported that silver particles exhibit efficient antifungal effects against Candida spp including *C. albicans*, *C. tropicalis*, *C. glabrata*, *C. krusei*,¹¹³⁻¹¹⁵.

3.8. Multiple organisms and systems

The actinobacterium, *Streptomyces minutiscleroticus* M10A62 biosynthesized Selenium (Se) was used to evaluate its anticancer (Hela, HepG2). It has also been investigated as a wound healing agent (as topic ointment) and antiviral drug against Dengue viruses in addition to its antioxidant and biofilm activity¹¹⁶. Another green biosynthesis approach was recently reported by Li et al. who used egg white, egg yolk, and serum to prepare gold nanoclusters (~5 nm) for efficient bioimaging of hepatocellular carcinoma cells¹¹⁷. These biosynthesized nanoparticles had excellent biocompatibility and low toxic effects on vital organs, i.e., liver, kidney, spleen, brain, heart, and lungs, which demonstrated their inertness.

Some of the biosynthesized silver nanoparticles from earthworm exudates were used against chloroquine sensitive and resistant malaria parasites, i.e., *Plasmodium falciparum*⁸⁷. Similarly, the silver nanoparticles biosynthesized from the nest of paper wasp (*Polistes* spp) was reported to possess antibacterial, antifungal, anticoagulant and blood clot dissolution properties¹¹⁸.

4. Outlook and conclusion

Biomedical applications of nanotechnology are dramatically increasing each year. However, the biocompatibility and the use of toxic compounds during the synthesis of nanoparticles are a matter of concern among the scientific and medical communities. The most important reservation regarding nanoscale materials in biomedical applications are toxicity, and adverse effects and genetic mutations due to the structural analogy of the particles to various cellular organelles. Moreover, the special selective barrier system within the body, i.e., the blood-brain barrier

and the blood-testis barrier cannot be easily crossed by pre-synthesized nanoparticles. Similarly, the biomedical application of nanoscale materials is highly dependent upon their sizes. For instance, nanomaterials of less than 10 nm size can easily be eliminated by the reticuloendothelial system within cells, whereas those above 100 nm size may cause a severe embolism in small capillaries.

The pre-synthesized materials may mimic autoimmune reactions due to their hydrophobic nature. Therefore, in situ biosynthesized nanoscale materials may avoid autoimmune reactions due to their locally restricted biosynthesis and rapid elimination. The pre-ionic solutions can easily pass through the blood-brain barrier which makes bioimaging in brain tissue a possibility. Formation of these materials takes advantage of the local neoplastic environment in case of cancer and elevated ROS levels in stroke, Parkinson's disease, and AD. The rapidly in situ biosynthesized nanoclusters (< 5 nm) can easily be eliminated from the body as compared to pre-synthesized nanoscale materials.

Similarly, all mammalian cells are secreting extracellular vesicles and exomes (i.e., 30- 150 nm size). The nanoclusters in situ biosynthesized within the tumor may also be secreted in the extracellular vesicles and exosomes and can thus be used as biomarkers for drug efficacy and tumor ablation after chemotherapy and bioimaging. Another possible opportunity in the nanomedicine is that biocompatible solutions such as Zn Gluconate can easily pass the placental barrier between the developing fetus and mother. This may provide an opportunity for preterm bioimaging or identify malformation, teratogeny or developing neoplasm inside the fetus.

The main bottleneck in the clinical application of nanoscale materials is that there still exists a gap from bench to bedside. This is partly due to the fact that most of the nanoscale materials are designed and fabricated by groups of chemists or chemical engineers, who, after preliminary in vitro experiments report their

results. And fewer studies report in vivo investigation for toxicity and adverse effects or even detailed clinical applications. The in situ biosynthesized nanoscale materials, and probes can readily be formed inside the body using local microenvironments. Therefore just a few additional parameters (regarding toxicity) may rule out possible toxic and adverse effects of such biosynthesized nanomaterials.

Herein, we conclude that the in situ biosynthesized nanoscale materials may provide a scaffold for safe, rapid, cost-effective, multimodal imaging and therapeutics of cancer, neurodegenerative and associated inflammatory ailments. Moreover, the green biosynthesis of these nanoscale materials may also help in reducing adverse environmental effects and health hazards.

Conflicts of interest

The authors declare that they have no conflict of interest.

Acknowledgment

This work is supported by National Key Research and Development Program of China (2017YFA0205300), National Natural Science Foundation of China (91753106, 21327902, 81325011 and 21675023) and the Fundamental Research Funds for the Central Universities, China. M. S. acknowledges support from the NSF-PREM program (NSF Award 1523588).

Notes and references

1. H. Shi, R. Magaye, V. Castranova and J. Zhao, *Part. Fibre Toxicol.*, 2013, 10, 15.
2. F. U. Rehman, C. Zhao, H. Jiang and X. Wang, *Biomater. Sci.*, 2016, 4, 40-54.
3. H.-S. Peng and D. T. Chiu, *Chem. Soc. Rev.*, 2015, 44, 4699-4722.
4. T. Yoshihara, Y. Hirakawa, M. Hosaka, M. Nangaku and S. Tobita, *J. Photoch. Photobio. C*, 2017, 30, 71-95.
5. R. A. Perez, S.-J. Choi, C.-M. Han, J.-J. Kim, H. Shim, K. W. Leong and H.-W. Kim, *Prog. Mater. Sci.*, 2016, 82, 234-293.
6. E. Katz and I. Willner, *Angew. Chem. Int. Ed.*, 2004, 43, 6042-6108.
7. R. I. MacCuspie, A. J. Allen and V. A. Hackley, *Nanotoxicology*, 2011, 5, 140-156.
8. K. Thorkelsson, P. Bai and T. Xu, *Nano Today*, 2015, 10, 48-66.
9. V. Dhand, L. Soumya, S. Bharadwaj, S. Chakra, D. Bhatt and B. Sreedhar, *Mater. Sci. Eng. C.*, 2016, 58, 36-43.
10. P. U. Rani and P. Rajasekharreddy, *Colloids Surf. Physicochem. Eng. Aspects*, 2011, 389, 188-194.
11. Z. Liu, M. A. Meyers, Z. Zhang and R. O. Ritchie, *Prog. Mater. Sci.*, 2017, 88, 467-498.
12. R. Mariselvam, A. Ranjitsingh, A. U. R. Nanthini, K. Kalirajan, C. Padmalatha and P. M. Selvakumar, *Spectrochim. Acta A*, 2014, 129, 537-541.
13. C. Krishnaraj, E. Jagan, S. Rajasekar, P. Selvakumar, P. Kalaichelvan and N. Mohan, *Colloids Surf. B. Biointerfaces*, 2010, 76, 50-56.
14. A. K. Mittal, Y. Chisti and U. C. Banerjee, *Biotechnol. Adv.*, 2013, 31, 346-356.
15. S. Irvani, *Green Chem.*, 2011, 13, 2638-2650.
16. K. N. Thakkar, S. S. Mhatre and R. Y. Parikh, *Nanomed. Nanotechnol. Biol. Med.*, 2010, 6, 257-262.
17. Y. Abboud, T. Saffaj, A. Chagraoui, A. El Bouari, K. Brouzi, O. Tanane and B. Hssane, *Appl. Nanosci.*, 2014, 4, 571-576.
18. E. P. Vetchinkina, E. A. Loshchinina, I. R. Vodolazov, V. F. Kursky, L. A. Dykman and V. E. Nikitina, *Appl. Microbiol. Biotechnol.*, 2016, 1-16.

19. H. Kato, *Nature Nanotechnology*, 2011, 6, 139-140.
20. R. Bhattacharya and P. Mukherjee, *Adv. Drug Del. Rev.*, 2008, 60, 1289-1306.
21. X. Zhang, S. Yan, R. Tyagi and R. Surampalli, *Chemosphere*, 2011, 82, 489-494.
22. I. Linkov, F. K. Satterstrom and L. M. Corey, *Nanomed. Nanotechnol. Biol. Med.*, 2008, 4, 167-171.
23. Y. Wang, A. Santos, A. Evdokiou and D. Losic, *J. Mater. Chem. B*, 2015, 3, 7153-7172.
24. Z. Tang, Y. Liu, M. He and W. Bu, *Angew. Chem. Int. Ed.*, 2018, <https://doi.org/10.1002/anie.201805664>.
25. S. Shaikh, F. u. Rehman, T. Du, H. Jiang, L. Yin, X. Wang and R. Chai, *ACS Appl. Mater. Interfaces*, 2018, 10, 26056-26063.
26. F. U. Rehman, T. Du, S. Shaikh, X. Jiang, Y. Chen, X. Li, H. Yi, J. Hui, B. Chen and M. Selke, *Nanomed. Nanotechnol. Biol. Med.*, 2018, <https://doi.org/10.1016/j.nano.2018.07.014>
27. P. Falagan-Lotsch, E. M. Grzincic and C. J. Murphy, *Proc. Natl. Acad. Sci. U.S.A.*, 2016, 113, 13318-13323.
28. J. Wang, G. Zhang, Q. Li, H. Jiang, C. Liu, C. Amatore and X. Wang, *Sci. Rep.*, 2013, 3, 1157.
29. Anshup, J. S. Venkataraman, C. Subramaniam, R. R. Kumar, S. Priya, T. S. Kumar, R. Omkumar, A. John and T. Pradeep, *Langmuir*, 2005, 21, 11562-11567.
30. A. Shamsaie, M. Jonczyk, J. D. Sturgis, J. P. Robinson and J. Irudayaraj, *J. Biomed. Opt.*, 2007, 12, 020502.
31. D. Trachootham, J. Alexandre and P. Huang, *Nat. Rev. Drug Discov.*, 2009, 8, 579-591.
32. C. Amatore, S. Arbault, M. Guille and F. Lemaitre, *Chem. Rev.*, 2008, 108, 2585-2621.
33. W. A. El - Said, H. Y. Cho, C. H. Yea and J. W. Choi, *Adv. Mater.*, 2014, 26, 910-918.
34. M. Husseiny, M. A. El-Aziz, Y. Badr and M. Mahmoud, *Spectrochim. Acta A*, 2007, 67, 1003-1006.
35. A. V. Singh, T. Jahnke, V. Kishore, B.-W. Park, M. Batuwangala, J. Bill and M. Sitti, *Acta Biomater.*, 2018, 71, 61-71.
36. T. Kunoh, M. Takeda, S. Matsumoto, I. Suzuki, M. Takano, H. Kunoh and J. Takada, *ACS Sustain. Chem. Eng.*, 2017, 6, 364-373.
37. D. Drescher, H. Traub, T. Büchner, N. Jakubowski and J. Kneipp, *Nanoscale*, 2017, 9, 11647-11656.
38. L. Lai, C. Zhao, X. Li, X. Liu, H. Jiang, M. Selke and X. Wang, *RSC Adv.*, 2016, 6, 30081-30088.
39. P. Faller, *Chem Bio Chem*, 2009, 10, 2837-2845.
40. A. Rauk, *Chem. Soc. Rev.*, 2009, 38, 2698-2715.
41. S. Chattoraj, M. Amin, S. Mohapatra, S. Ghosh and K. Bhattacharyya, *Chemphyschem*, 2016, 17, 61-68.
42. S. Gao, D. Chen, Q. Li, J. Ye, H. Jiang, C. Amatore and X. Wang, *Sci. Rep.*, 2014, 4, 4384.
43. M. J. Piao, K. A. Kang, I. K. Lee, H. S. Kim, S. Kim, J. Y. Choi, J. Choi and J. W. Hyun, *Toxicol. Lett.*, 2011, 201, 92-100.
44. J.-C. G. Bünzli, *Chem. Rev.*, 2010, 110, 2729-2755.
45. B. C. Heng, G. K. Das, X. Zhao, L.-L. Ma, T. T.-Y. Tan, K. W. Ng and J. S.-C. Loo, *Biointerphases*, 2010, 5, FA88-FA97.
46. Y. Zheng, J. Lin, Y. Liang, Q. Lin, Y. Yu, C. Guo, S. Wang and H. Zhang, *Mater. Lett.*, 2002, 54, 424-429.

47. L. J. Charbonnière, R. Ziessel, M. Montalti, L. Prodi, N. Zaccheroni, C. Boehme and G. Wipff, *J. Am. Chem. Soc.*, 2002, 124, 7779-7788.
48. J. Ye, J. Wang, Q. Li, X. Dong, W. Ge, Y. Chen, X. Jiang, H. Liu, H. Jiang and X. Wang, *Biomater. Sci.*, 2016, 4, 652-660.
49. G. C. Han and Y. N. Liu, *Luminescence*, 2010, 25, 389-393.
50. R. Hänsch and R. R. Mendel, *Curr. Opin. Plant Biol.*, 2009, 12, 259-266.
51. D. Mahanand and J. Houck, *Clin. Chem.*, 1968, 14, 6-11.
52. D. W. Domaille, E. L. Que and C. J. Chang, *Nat. Chem. Biol.*, 2008, 4, 168-175.
53. W. Chyan, D. Y. Zhang, S. J. Lippard and R. J. Radford, *Proc. Natl. Acad. Sci. U.S.A.*, 2014, 111, 143-148.
54. J. R. Cantor and D. M. Sabatini, *Cancer Discov.*, 2012, 2, 881-898.
55. C. V. Dang, *Genes Dev.*, 2012, 26, 877-890.
56. M. Su, J. Ye, Q. Li, W. Ge, Y. Zhang, H. Jiang, C. Amatore and X. Wang, *RSC Advances*, 2015, 5, 74844-74849.
57. K.-M. Kim, M.-K. Kim, H.-J. Paek, S.-J. Choi and J.-M. Oh, *Colloids Surf. B. Biointerfaces*, 2016, 145, 870-877.
58. T. Du, C. Zhao, F. ur Rehman, L. Lai, X. Li, Y. Sun, S. Luo, H. Jiang, M. Selke and X. Wang, *Nano Res.*, 2017, 10, 2626-2632.
59. L. Lai, C. Zhao, M. Su, X. Li, X. Liu, H. Jiang, C. Amatore and X. Wang, *Biomater. Sci.*, 2016, 4, 1085-1091.
60. C. Zhao, L. Lai, F. U. Rehman, C. Qian, G. Teng, H. Jiang and X. Wang, *RSC Adv.*, 2016, 6, 110525-110534.
61. Y.-Z. Wu, J. Sun, H. Yang, X. Zhao, D. He, M. Pu, G. Zhang, N. He and X. Zeng, *ACS Appl. Mater. Interfaces*, 2018, 10 105-113.
62. X. Liu, H. Jiang, J. Ye, C. Zhao, S. Gao, C. Wu, C. Li, J. Li and X. Wang, *Adv. Funct. Mater.*, 2016, 26, 8694-8706.
63. Y.-X. J. Wang, S. M. Hussain and G. P. Krestin, *Eur. Radiol.*, 2001, 11, 2319-2331.
64. C. G. Hadjipanayis, M. J. Bonder, S. Balakrishnan, X. Wang, H. Mao and G. C. Hadjipanayis, *Small*, 2008, 4, 1925-1929.
65. Y.-w. Jun, J.-w. Seo and J. Cheon, *Acc. Chem. Res.*, 2008, 41, 179-189.
66. J.-H. Lee, Y.-M. Huh, Y.-w. Jun, J.-w. Seo, J.-t. Jang, H.-T. Song, S. Kim, E.-J. Cho, H.-G. Yoon and J.-S. Suh, *Nat. Med.*, 2007, 13, 95-99.
67. C. Xu, J. Xie, D. Ho, C. Wang, N. Kohler, E. G. Walsh, J. R. Morgan, Y. E. Chin and S. Sun, *Angew. Chem.*, 2008, 120, 179-182.
68. J.-s. Choi, Y.-w. Jun, S.-I. Yeon, H. C. Kim, J.-S. Shin and J. Cheon, *J. Am. Chem. Soc.*, 2006, 128, 15982-15983.
69. H. B. Na, I. C. Song and T. Hyeon, *Adv. Mater.*, 2009, 21, 2133-2148.
70. N. Singh, G. S. Jenkins, R. Asadi and S. Doak, *Nano Rev.*, 2010, 1, 5358.
71. C. Zhao, T. Du, L. Lai, X. Liu, X. Jiang, X. Li, Y. Chen, H. Zhang, Y. Sun and S. Luo, *Small*, 2016, 12, 6255-6265.
72. T. Du, C. Zhao, L. Lai, X. Li, Y. Sun, S. Luo, H. Jiang, N. Gu, M. Selke and X. Wang, *Adv. Funct. Mater.*, 2017, 27, 1603926.
73. R. Mahlberg, S. Lorenzen, P. Thuss-Patience, V. Heinemann, P. Pfeiffer and M. Möhler, *Chemotherapy*, 2017, 62, 62-70.

74. M. F. Osborn, J. D. White, M. M. Haley and V. J. DeRose, *ACS Chem. Biol.*, 2014, 9, 2404.
75. Y. Min, J. Li, F. Liu, E. K. Yeow and B. Xing, *Angew. Chem.*, 2014, 126, 1030-1034.
76. S. Mazumder, R. Dey, M. Mitra, S. Mukherjee and G. Das, *J Nanomater.*, 2009, 2009, 38.
77. C. de Jong, S. Sanders, G. Creemers, A. Burylo, M. Taks, J. Schellens and M. Deenen, *Br. J. Clin. Pharmacol.*, 2017.
78. D. Zhang, J. Pan, X. Xiang, Y. Liu, G. Dong, M. J. Livingston, J.-K. Chen, X.-M. Yin and Z. Dong, *J. Am. Soc. Nephrol.*, 2017, 28, 1131-1144.
79. D. Chen, C. Zhao, J. Ye, Q. Li, X. Liu, M. Su, H. Jiang, C. Amatore, M. Selke and X. Wang, *ACS Appl. Mater. Interfaces*, 2015, 7, 18163-18169.
80. F. U. Rehman, C. Zhao, C. Wu, X. Li, H. Jiang, M. Selke and X. Wang, *Nano Res.*, 2016, 9, 3305-3321.
81. E. Larios-Rodriguez, C. Rangel-Ayon, S. Castillo, G. Zavala and R. Herrera-Urbina, *Nanotechnology*, 2011, 22, 355601.
82. M. Gillan and N. Zander, *In-vitro Synthesis of Gold Nanoclusters in Neurons*, US Army Research Laboratory Aberdeen Proving Ground United States, 2016, Accession no AD1008573, <http://www.dtic.mil/dtic/tr/fulltext/u2/1008573.pdf>
83. A. L. West, N. M. Schaeublin, M. H. Griep, E. I. Maurer-Gardner, D. P. Cole, A. M. Fakner, S. M. Hussain and S. P. Karna, *ACS Appl. Mater. Interfaces*, 2016, 8, 21221-21227.
84. A. Elfick, G. Rischitor, R. Mouras, A. Azfer, L. Lungaro, M. Uhlarz, T. Herrmannsdörfer, J. Lucocq, W. Gamal and P. Bagnaninchi, *Sci. Rep.*, 2017, 7, 39755.
85. J. A. MacKay, M. Chen, J. R. McDaniel, W. Liu, A. J. Simnick and A. Chilkoti, *Nature materials*, 2009, 8, 993-999.
86. J. Anitha and I. A. Jayraaj, *World J Pharm Pharm Sci*, 2013, 2, 4917-4928.
87. A. Jaganathan, K. Murugan, C. Panneerselvam, P. Madhiyazhagan, D. Dinesh, C. Vadivalagan, B. Chandramohan, U. Suresh, R. Rajaganesh and J. Subramaniam, *Parasitol. Int.*, 2016, 65, 276-284.
88. V. Kathiravan, S. Ravi and S. Ashokkumar, *Spectrochim. Acta A*, 2014, 130, 116-121.
89. T. Muthukumar, B. Sambandam, A. Aravinthan, T. P. Sastry and J.-H. Kim, *Process Biochem.*, 2016, 51, 384-391.
90. R. Sankar, R. Maheswari, S. Karthik, K. S. Shivashangari and V. Ravikumar, *Mater. Sci. Eng. C*, 2014, 44, 234-239.
91. S. Iram, S. Khan, A. A. Ansary, M. Arshad, S. Siddiqui, E. Ahmad, R. H. Khan and M. S. Khan, *Spectrochim. Acta A*, 2016, 168, 123-131.
92. F. U. Rehman, C. Zhao, H. Jiang, M. Selke and X. Wang, *Photodiagnosis Photodyn. Ther.*, 2016, 13, 267-275.
93. F. U. Rehman, C. Zhao, C. Wu, H. Jiang, M. Selke and X. Wang, *RSC Adv*, 2015, 5, 107285-107292.
94. C. Zhao, F. Ur Rehman, Y. Yang, X. Li, D. Zhang, H. Jiang, M. Selke, X. Wang and C. Liu, *Sci. Rep.*, 2015, 5, 11518.
95. T. J. Dougherty, C. J. Gomer, B. W. Henderson, G. Jori, D. Kessel, M. Korbelik, J. Moan and Q. Peng, *J. Natl. Cancer Inst.*, 1998, 90, 889-905.
96. A. Heinrichs, *Nat. Cell Biol.*, 2009, 11, S7.
97. J. M. Nicholls, L. L. Poon, K. C. Lee, W. F. Ng, S. T. Lai, C. Y. Leung, C. M. Chu, P. K. Hui, K. L. Mak and W. Lim, *Lancet*, 2003, 361, 1773-1778.
98. H. Cook, *J. Clin. Pathol.*, 1997, 50, 716.
99. J. A. Thomas, *Chem. Soc. Rev.*, 2015, 44, 4494-4500.

100. A. J. Amoroso and S. J. Pope, *Chem. Soc. Rev.*, 2015, 44, 4723-4742.
101. X. Qian and Z. Xu, *Chem. Soc. Rev.*, 2015, 44, 4487-4493.
102. T. D. Ashton, K. A. Jolliffe and F. M. Pfeffer, *Chem. Soc. Rev.*, 2015, 44, 4547-4595.
103. T. Buerki-Thurnherr, K. Schaepper, L. Aengenheister and P. Wick, *Chem. Res. Toxicol.*, 2018, 31, 641-642.
104. S. Sharifi, S. Behzadi, S. Laurent, M. L. Forrest, P. Stroeve and M. Mahmoudi, *Chem. Soc. Rev.*, 2012, 41, 2323-2343.
105. T.-M. Liu, J. Conde, T. Lipiński, A. Bednarkiewicz and C.-C. Huang, *Prog. Mater. Sci.*, 2017, 88, 89-135.
106. M. J. Hajipour, K. M. Fromm, A. A. Ashkarran, D. J. de Aberasturi, I. R. de Larramendi, T. Rojo, V. Serpooshan, W. J. Parak and M. Mahmoudi, *Trends Biotechnol.*, 2012, 30, 499-511.
107. C. Kaweeteerawat, A. Ivask, R. Liu, H. Zhang, C. H. Chang, C. Low-Kam, H. Fischer, Z. Ji, S. Pokhrel and Y. Cohen, *Environ. Sci. Technol.*, 2015, 49, 1105-1112.
108. V. S. Kumar, B. Nagaraja, V. Shashikala, A. Padmasri, S. S. Madhavendra, B. D. Raju and K. R. Rao, *J. Mol. Catal. A: Chem.*, 2004, 223, 313-319.
109. N. Shinde, A. Lokhande and C. Lokhande, *J. Photochem. Photobiol. B: Biol.*, 2014, 136, 19-25.
110. P. Velmurugan, K. Anbalagan, M. Manosathyadevan, K.-J. Lee, M. Cho, S.-M. Lee, J.-H. Park, S.-G. Oh, K.-S. Bang and B.-T. Oh, *Bioprocess Biosystems Eng.*, 2014, 37, 1935-1943.
111. V. Gopinath and P. Velusamy, *Spectrochim. Acta A*, 2013, 106, 170-174.
112. V. Kathiravan, S. Ravi, S. Ashokkumar, S. Velmurugan, K. Elumalai and C. P. Khatiwada, *Spectrochim. Acta A*, 2015, 139, 200-205.
113. E. J. J. Mallmann, F. A. Cunha, B. N. Castro, A. M. Maciel, E. A. Menezes and P. B. A. Fachine, *Rev. Inst. Med. Trop. Sao Paulo*, 2015, 57, 165-167.
114. J. J. A. Bonilla, D. J. P. Guerrero, C. I. S. Suárez, C. C. O. López and R. G. T. Sáez, *World J. Microbiol. Biotechnol.*, 2015, 31, 1801-1809.
115. L. S. Devi and S. R. Joshi, *J. Microbiol.*, 2014, 52, 667-674.
116. S. Ramya, T. Shanmugasundaram and R. Balagurunathan, *J. Trace Elem. Med. Biol.*, 2015, 32, 30-39.
117. L. Li, X. Liu, C. Fu, L. Tan and H. Liu, *Opt. Commun.*, 2015, 355, 567-574.
118. A. Lateef, M. A. Akande, S. A. Ojo, B. I. Folarin, E. B. Gueguim-Kana and L. S. Beukes, *3 Biotech*, 2016, 6, 1-10.